第33卷第11期 焊 接 学 报 Vol. 33 No. 11
2012年11月 TRANSACTIONS OF THE CHINA WELDING INSTITUTION November 2012

不锈钢超高频直流脉冲 GTAW 焊缝成形行为

杨明轩[1]， 齐铂金[1]， 从保强[1]， 李 伟[1,2]， 杨 舟[1]
(1. 北京航空航天大学 机械工程及自动化学院，北京 100191;
2. 北京石油化工学院 电气工程系，北京 102617)

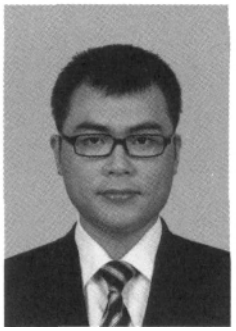
杨明轩

摘 要：基于超高频直流脉冲钨极氩弧焊技术(UHF-GTAW，ultrahigh frequency pulse-gas tungsten arc welding)，完成了0Cr18Ni9Ti奥氏体不锈钢焊缝熔透特性试验，研究分析了超高频脉冲方波电流对焊缝成形及熔池金属流动的影响规律. 结果表明，在高频脉冲电流作用下，熔透率随频率增加而增大，在同等平均电流条件下，当脉冲频率达到80 kHz时，熔宽减小，熔深最大增加了88.7%，熔透率显著提升，至少增大了24.6%以上. 结合试验数据对熔池流动行为进行了理论分析，讨论了熔池内部电磁力对焊缝成形的作用及对流体的驱动效果.

关键词：超高频直流脉冲 GTAW；焊缝成形；熔池流动行为
中图分类号：TG403 **文献标识码**：A **文章编号**：0253-360X(2012)11-0031-04

0 序 言

直流钨极氩弧焊是奥氏体不锈钢的常用焊接方法，其焊接过程稳定，但焊缝熔深较浅，熔透率较低[1]. 目前有诸如添加活性剂、复合超声及高频脉冲焊接等方法以提高焊缝熔透率，其中高频脉冲焊接作为一种新工艺正得到越来越广泛的应用，该工艺的焊缝成形及熔池流动一直是学界研究的重点.

脉冲电流焊接时，较大的电弧力可促进熔池金属流动，引起熔池表面凹陷，热源下移，熔深增大. 研究结果证明[2]，熔池金属流动的驱动力主要有浮力、电磁力、表面张力和等离子流力，其在熔池内部驱动液态金属流动，对熔池流动状态起重要作用，直接决定熔池形貌，电磁力和表面张力是熔池流动的主要驱动力[3,4]，将产生双环流流动模式，共同影响焊缝成形[5].

目前，针对高频脉冲焊接焊缝成形及熔池流动的研究尚不足，文中基于超高频直流脉冲钨极氩弧焊技术(UHF-GTAW，ultrasonic frequency pulse-gas tungsten arc welding)进行了0Cr18Ni9Ti奥氏体不锈钢熔透特性试验，初步分析了UHF-GTAW熔池流动行为及脉冲电流对其熔透特性的作用规律，对研究UHF-GTAW熔池行为具有重要意义.

收稿日期：2011-08-05
基金项目：国家自然科学基金资助项目(50975015)

1 试验方法

0Cr18Ni9Ti奥氏体不锈钢，板厚5 mm，规格为150 mm×60 mm，焊前经砂纸打磨和酒精清洗；电极直径为2.4 mm铈钨W-2% Ce；保护气体为99.99%普通氩气，流量12 L/min，焊接速度为120 mm/min，焊缝长度为100～120 mm. 试验过程中焊接平均电流值计算公式如式(1)，脉冲电流参数如表1，其中1～7组钨极顶端与工件表面距离3 mm，8，9组距离5 mm.

$$I_{avg}=(1-\delta)\times I_b+\delta\times I_p \quad (1)$$

式中：I_b 为基值电流；I_p 为峰值电流；t_b，t_p 分别为基值电流及峰值电流作用时间；脉冲电流占空比 $\delta=t_p/(t_b+t_p)$.

表1 0Cr18Ni9Ti奥氏体不锈钢焊接电流参数
Table 1 Parameters of welding current for 0Cr18Ni9Ti

试验号	基值电流 I_b/A	峰值电流 I_p/A	平均电流 I_{avg}/A	脉冲频率 f/kHz	占空比 δ(%)
1	80	160	120	10	50
2	80	160	120	20	50
3	80	160	120	40	50
4	80	160	120	80	50
5	60	135	120	10	80
6	60	135	120	20	80
7	60	135	120	40	80
8	100	180	140	10	50
9	100	180	140	40	50

2 试验结果与讨论

2.1 焊缝熔透特性

在上节所述的试验条件下获得表 1 中各组参数所对应的焊件，其中 1 ~ 4 号焊缝成形如图 1 所示，1 ~ 9 号焊缝成形参数如表 2 及图 2 所示.

表 2 0Cr18Ni9Ti 奥氏体不锈钢焊缝熔透特性

Table 2 Welds penetration for 0Cr18Ni9Ti by UHF-GTAW

试验号	熔宽 B/mm	熔深 H/mm	熔透率 Ψ(%)	弧长 L/mm
1	5.03	1.41	28.1	3
2	5.56	2.01	36.2	3
3	6.19	2.80	45.2	3
4	4.72	2.66	56.3	3
5	5.81	2.50	43.1	3
6	5.06	2.38	47.0	3
7	5.62	2.72	48.5	3
8	6.50	2.62	40.3	5
9	6.80	3.26	47.9	5

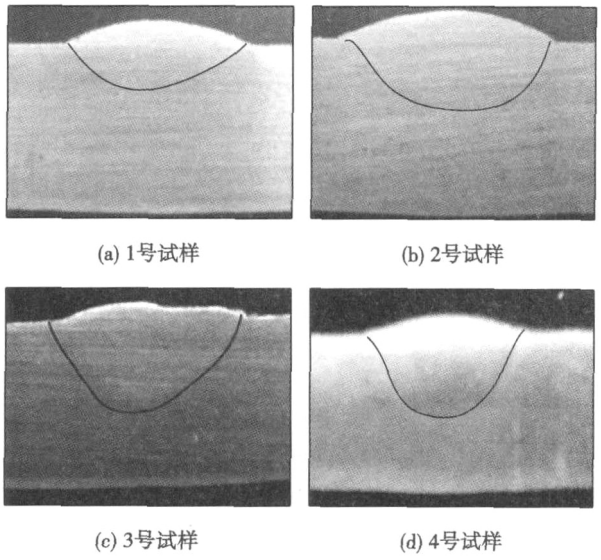

(a) 1号试样 (b) 2号试样

(c) 3号试样 (d) 4号试样

图 1 焊缝成形

Fig. 1 Appearance for welds

由图 1，图 2 可知，随着脉冲频率的增大，焊缝熔深在 40 kHz 以下频率段增加，而后小幅回落，熔宽的变化趋势与之相似，熔透率提高，当脉冲频率为 80 kHz 时(4 号试样)，焊缝熔宽减小，与 1 号试样相比，熔深增加了 88.7%，熔透率增大了 100.4%. 分析认为，随着脉冲频率的升高，电弧收缩效应增强，在 80 kHz 的频率水平下，电弧收缩最为显著，电弧作用面积减小，能量集中，电弧挺度提高，穿透性增强，熔宽减小，因此熔透率提高.

选取脉冲频率分别为 10，20，40 kHz 的 1 ~ 3 号及 5 ~ 7 号作为对比试验，其中前者占空比为 50%，后者为 80%，如图 3 所示.

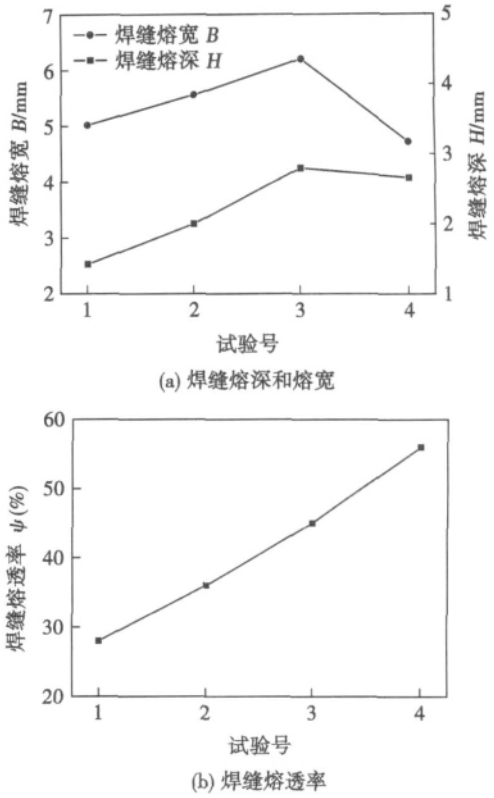

图 2 焊缝熔透成形

Fig. 2 Parameters of welds appearance

由图 3 可知，当占空比为 80% 时，随着脉冲频

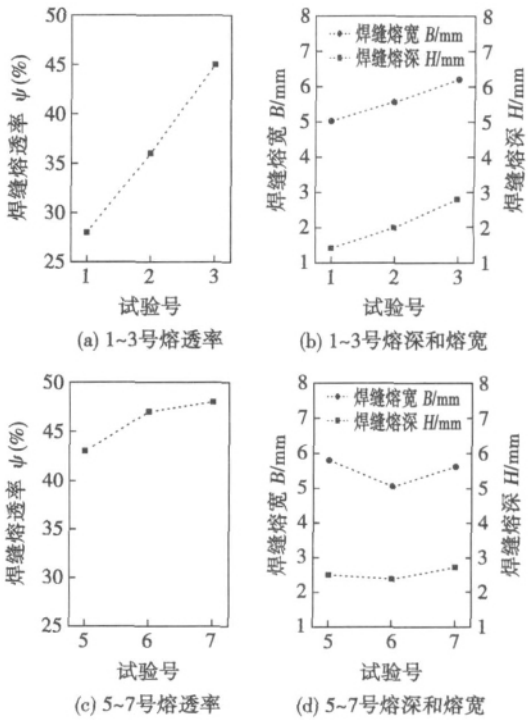

图 3 焊缝熔透成形(对比试验)

Fig. 3 Parameters of welds appearance

率的增加，熔透率在一定范围内呈现小幅增长趋势，与图 2a 类似，熔深、熔宽随频率的变化趋势基本相同，但与 50% 占空比相比，其波动较小，即在占空比较大时，由于脉冲电流幅值减小，焊缝熔透特性参数随脉冲频率变化敏感性降低. 由作者已完成的电弧力测量试验数据可知[8]，占空比 50% 时，随脉冲频率的增大，其电弧力呈显著上升趋势，并在 80 kHz 时达到最大值，而占空比较大时其电弧力波动范围较小，基本处于恒定状态. 由于电弧力可造成熔池表面凹陷，电弧力越大其凹陷越明显，热源下降越显著，电弧穿透力增强，呈现出熔深增大、熔透率显著提升的成形效果[7]，这与图 3 反映的试验结果相符.

改变弧长进一步考查 8，9 号试样（弧长为 5 mm），如图 4 所示. 脉冲频率为 40 kHz 时，熔深达到试验所得最大值，其熔深增加了 16.4% 以上，与同等弧长下为 10 kHz 时相比增大了 24.4%，熔透率增加了 18.9%，但由于 8，9 号试样平均电流较大，熔宽整体水平与 1 ~ 7 号试样相比明显增大，故与之相比，熔透率并未出现明显提升.

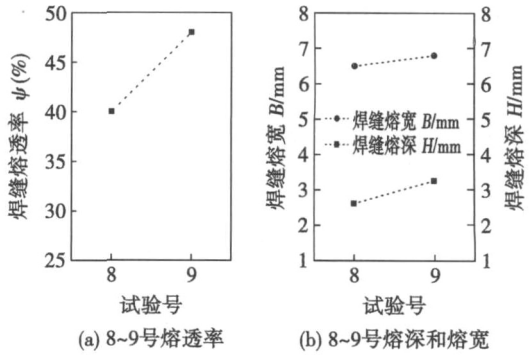

图 4　焊缝熔透成形（弧长为 5 mm）

Fig. 4　Parameters of welds appearance

2.2　熔池流动行为分析

电弧所产生的轴向压力作用于熔池表面，如 2.1 节所述，将使熔池表面出现凹陷，造成热源下移，增强电弧穿透性，故熔深增大；熔池内部液态金属的流动主要依靠浮力、表面张力、自激搅拌电磁力，如图 5 所示，焊接方向垂直于纸面，其中表面张力为表面力，电磁力和浮力为体积力. 其中，J 为电流密度，B 为磁场强度，$J\times B$ 为电磁力，d 为工作厚度，Z 为轴向，R 为径向.

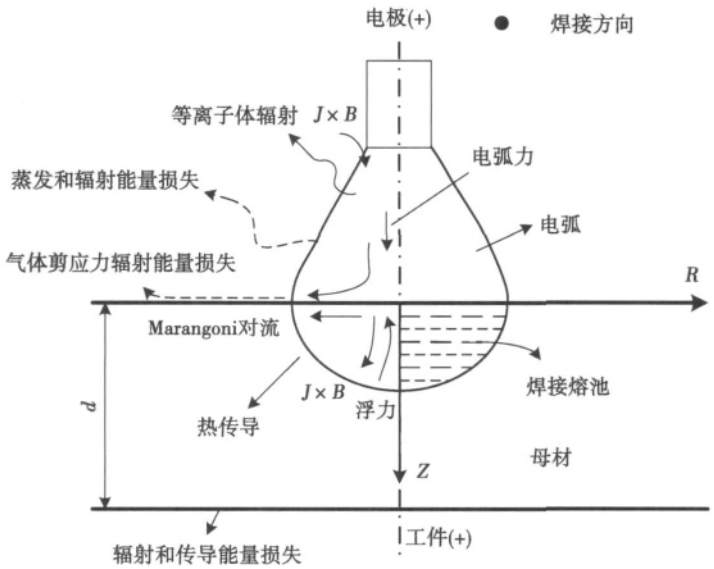

图 5　熔池驱动力示意图

Fig. 5　Schematic diagram of driving forces for weld pool

与浮力相比，电磁力对熔池的驱动强度及流体运动速度均占主导地位[8]，熔池在其作用下呈现表面中心聚集、内部向下深入的流动模式[9]，由于强电磁力将影响流体流动，增强电弧作用面积下熔池的渗透能力[10]，故与电弧轴向电磁力及等离子流力相比，通过控制熔池流动方式以增加熔深、提高焊缝熔透率. 文献 [7] 指出，在半球形熔池的任一横截面上均存在电磁力驱动的表面中心聚集、内部向下深入环流，该环流所在平面与电弧轴向平行，这种环流的相互作用可将其部分动能转化为熔池绕电弧轴线的圆周运动，即周向搅拌，如图 6 所示，这将进一步促进熔池流动. 由于电磁力随频率的增加而增大[11]，故 UHF-GTAW 将产生更大的搅拌电磁力，则

熔池金属向下流动的趋势随之增强，沿电弧轴向的周向环流亦增大，电磁搅拌增强[12]，熔池流动性提高. Marangoni 对流将使熔池金属由中心向边缘呈辐射状流动，易形成浅而宽的焊缝，但其流速大，增强了熔池流动性.

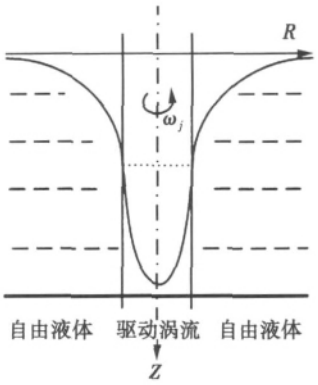

图 6 电磁力搅拌模型

Fig. 6 Model of forced vortex in weld pool

如前所述的由电磁力及表面张力所驱动的两个方向相反的环流在熔池中共存，并共同决定熔池形貌，在常规情况下，两个环流在熔池中呈上下分层状态，如图 7a 所示，熔池表面由表面张力主导决定熔宽，电磁力作用增加熔深，该模式具有普适性，常规 GTAW 时，电磁力强度弱，熔池在表面张力驱动下易形成浅而宽的焊缝; 加入脉冲电流后，电磁力作用增强，熔池向下趋势明显，当频率达到 40 kHz 以上时，两个环流的分布如图 7b 所示，熔池中心电磁力驱动效应占主导地位，液态金属向下流动显著增大，该流动状态有利于提高熔透率，并与 Marangoni 对流综合作用，显著增强熔池流动性.

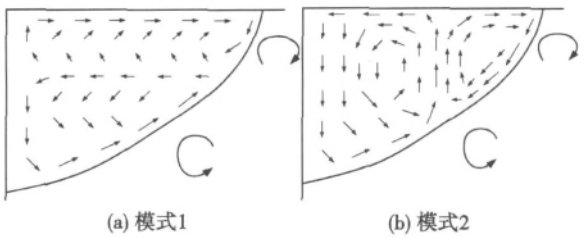

图 7 熔池双环流运动模型

Fig. 7 Model of double-circumfluence in weld pool

3 结 论

(1) 随着脉冲频率的增加，UHF-GTAW 熔宽、熔深增长趋势相似，熔透率上升趋势明显，在较高频率下(f>40 kHz)，熔深及熔透率显著增大.

(2) 采用 UHF-GTAW 在较大脉冲频率下，熔池内部电磁力增大，所驱动的环流强度增强，促进了熔池流动并有利于形成深而窄的焊缝成形.

参考文献:

[1] 杨春利. 电弧焊基础[M]. 哈尔滨: 哈尔滨工业大学出版社，2003.

[2] Kim W H, Fan H G, Na S J. Effect of various driving forces on heat and mass transfer in arc welding [J]. Numerical Heat Transfer, Part A: Applications, 1997, 32: 6, 633-652.

[3] KumarA, DebRoy T. Calculation of three-dimensional electromagnetic force field during arc welding [J]. Journal of Applied Physics, 2003, 2(94): 1267-1277.

[4] 李志宁，都 东，常保华，等. 激光-等离子弧复合焊接熔池流动和传热的数值模拟[J]. 焊接学报，2007，28(7)：37-40.
Li Zhining, Du Dong, Chang Baohua, *et al*. Numerical simulation on flow and heat transfer in weld pool of laser-plasma hybrid welding [J]. Transactions of the China Welding Institution, 2007, 28(7): 37-40.

[5] Kou S, Sun D K. Fluid flow and weld penetration in stationary arc weld [J]. Metallurgical Transaction A, 1985, 16 A: 203-213.

[6] 杨明轩，齐铂金，从保强，等. 脉冲电流参数对奥氏体不锈钢电弧行为的影响[J]. 焊接学报，2012，33(10)：67-70.
Yang Mingxuan, Qi Bojin, Cong Baoqiang, *et al*. The influence of pulse current parameters on arc behavior by austenite stainless steel [J]. Transactions of the China Welding Institution, 2012, 33(10): 67-70.

[7] LinM L, Eagar T W. Influence of arc pressure on weld pool geometry [J]. Welding Journal, 1985, 64(6): 162s-169s.

[8] Oreper G M, Eagar T W. Convection in arc weld pools [J]. Welding Journal, 1983, 62(11): 307s-312s.

[9] Tsai M C, Kou S. Electromagnetic force induced convection in weld pool with a free surface: A model is developed to predict heat transfer, fluid flow and pool shape in GTAW [J]. Welding Journal, 1990, 69(6): 241s-246s.

[10] Zacharia, David. Weld pool development during GTA and laser beam welding of type 304 stainless steel, Part I-Theoretical analysis [J]. Welding Journal, 1989, 68(12): 499s-509s.

[11] 从保强，齐铂金，周兴国. 超快变换高频变极性方波 TIG 电弧行为[J]. 焊接学报，2009(6)：87-90.
Cong Baoqiang, Qi Bojin, Zhou Xingguo. TIG arc behavior of ultra fast-convert high-frequency variable polarity square wave [J]. Transactions of the China Welding Institution, 2009(6): 87-90.

[12] Atthey D R. A mathematical model for fluid flow in a weld pool at high currents [J]. Journal of Fluid Mechanics, 1980, 98(4): 787-801.

作者简介： 杨明轩，男，1985 年出生，博士研究生. 主要从事高频脉冲氩弧焊电弧及接头组织性能研究. 发表论文 4 篇. Email: oybenq@gmail.com.

通讯作者： 齐铂金，男，教授. Email: qbj@buaa.edu.cn

remelted sample had higher hardness, better wear resistance than the as-sprayed coating.

Key words: laser remelting; plasma spraying; Ni-based coating; WC particles reinforced

Parametric modeling and vector graphics plotting for welding joint groove SHEN Chunlong[1,2], YU Jingbao[2], PENG Yong[2], WANG Kehong[2] (1. Dept. Mechanical & Electrical Engineering, Taizhou Teacher College, Taizhou 225300, China; 2. School of Material Science & Engineering, Nanjing University Science & Technology, Nanjing 210094, China). pp 17-20

Abstract: Parametric description and graphics plotting of welding joint groove play an important role for software development of welding process design. Parametric model of joint type and groove graphics is presented based on double U-groove. Principle for joint groove graphics parameter-driven is analyzed and the function of geometry parameter dynamic labeling for groove graphics is realized. The classes for primitives plotting object-oriented are presented. The primitives-data storage structure of parameter plotting process is showed. The use of picking primitive object with mouse resolves the question of modifying the primitive properties. The generation of neutral vector WMF file and serialization process for joint graphics are discussed. The results show that parametric model and vector plotting for joint groove graphics can handle labeling for joint parameter and embed graphics distortion in report form.

Key words: joint groove; parametric modeling; vector graphics; parameter-driven

Effect of premelting oxide layer on AA-TIG weld shape FAN Ding[1,2], KANG Zaixiang[2], HUANG Yong[1,2], Yan Liqin[2], WANG Xinxin[2], HAO Zhenni[2] (1. State Key Laboratory of Gansu Advanced Non-ferrous Metal Materials, Lanzhou University of Technology, Lanzhou 730050, China; 2. Key Laboratory of Non-ferrous Metal Alloys, The Ministry of Education, Lanzhou University of Technology, Lanzhou 730050, China). pp 21-25

Abstract: AA-TIG welding is a new and efficient welding process before which pre-melting oxide layer was prepared on weld position by low current assisting arc with $Ar+O_2$ as shield gas. As a result, a deep and narrow weld bead can be obtained. In this experiment, through turning the assisting arc parameters to change the thickness of oxide layer, the influence of the thick of oxide layer on stainless steel weld formation was analyzed. The results show that the parameters of assisting arc have great effect on the thickness of oxide layer, the oxide layer becomes thicker when the oxygen gas flow rate or the heat input of assisting arc increase. And the thickness of oxide layer influences the weld depth/width ratio, the weld depth/width ratio climbs up at first and then declines with the increase of the thickness of oxide layer.

Key words: stainless steel; AA-TIG welding; oxide layer; weld shape

Effect of temperature on CO_2 corrosion of dissimilar weld joint WANG Jing[1], LU Minxu[1], YANG Ping[1], ZHANG Lei[1], CHANG Wei[2] (1. School of Materials Science and Engineering, University of Science and Technology Beijing, Beijing 100083, China; 2. China National Offshore Oil Corp. (CNOOC) Research Center, Beijing 100027, China). pp 26-30

Abstract: To study the effect of temperature on CO_2 corrosion behavior of dissimilar weld joint, dissimilar weld joint of X70 pipeline steel and 2250 duplex stainless steel welded by metal inertia gas welding was used experimentally. Microstructure of X70/weld joint interface and CO_2 corrosion morphologies in weld joint at different temperatures were observed and analyzed. The results showed that dendritic structure appeared in weld joint. Narrow fusion zone and type Ⅱ boundary existed between micro-alloy steel and weld joint, and obvious concentration gradient of Ni and Cr elements was observed. Serious corrosion occurred in HAZ of micro-alloy at high temperature other than at low temperature. Corrosion product on surface of micro-alloy was shown loose while that on surface of weld joint was shown compact. Such different corrosion tendency of micro-alloy and weld joint was probably caused by the different ionic migration ratios as a result of different corrosion potentials of metals and different temperatures.

Key words: temperature; dissimilar weld joint; microstructure; corrosion rate; mechanism

Weld appearance behavior in welding pool of stainless steel by ultrahigh frequency pulse GTAW process YANG Mingxuan[1], QI Bojin[1], CONG Baoqiang[1], LI Wei[1,2], YANG Zhou[1] (1. School of Mechanical Engineering and Automation, Beihang University, Beijing 100191, China; 2. Beijing Institute of Petrochemical Technology, Beijing 100191, China). pp 31-34

Abstract: Based on ultrahigh frequency pulse gas tungsten arc welding process for stainless steel, appearance of weld and the influence of pulse current to flow in welding pool were carried out. The experimental results show that the welds penetration increased with the increasing of pulse frequency. When the pulse frequency $f=80$ kHz, the weld penetration rose by 24.6% at least with the depth increased by 88.7% at most. It could also be found that the width and depth of weld had the similar trend with the changed pulse frequency. Based on the data from experiments, the flow movement in the pool was investigated with effect of electromagnetic force to weld appearance and forced flow as the main purpose.

Key words: ultrahigh frequency pulse GTAW process; appearance of weld; flow behavior of welding pool

A new weld shaping method with trailing impact rolling and tensile and fatigue properties for equal load-carrying capacity joints WANG Jiajie[1,2], YANG Jianguo[3], ZHANG Jingqiang[1], DONG Zhibo[1], FANG Hongyuan[1], GANG Tie[1] (1. State Key Laboratory of Advanced Welding and Joining, Harbin Institute of Technology, Harbin 150001, China; 2. School of Materials and Chemical Engineering, Heilongjiang Institute of Technology, Harbin 150050, China; 3. Institute of Process Equipment and Control Engineering, Zhejiang University of Technology, Hangzhou 310014, China). pp 35-38